

## Mobility of two-dimensional electrons in an AlGaIn/GaN modulation-doped heterostructure

Sibel Gökden\*

Department of Physics, Balıkesir University, Balıkesir, Turkey

Received 26 June 2003, revised 24 September 2003, accepted 29 September 2003

Published online 19 November 2003

PACS 72.20.Dp, 73.40.Kp

The results of experimental and theoretical studies concerning the temperature dependence of electron mobility in a two-dimensional electron gas (2DEG) confined near the interface of an AlGaIn/GaN heterostructure are presented. In order to compare the experimental results with the theory a simple analytical formula is used for the low-field electron mobility, which uses the 2D degenerate statistics for a 2DEG confined in a triangular well. All standard scattering mechanisms, including scattering by acoustic and optical phonons, remote and background impurities and interface roughness (IFR), have been included in the calculations. From the calculated dependence of mobility on temperature, it is clear that IFR and ionised impurity scattering dominate the low-temperature mobility of 2D electrons in AlGaIn/GaN structures with a high electron density  $n_s > 10^{12} \text{ cm}^{-2}$ . At intermediate temperatures, acoustic deformation potential and piezoelectric scattering are the dominant mechanisms. The polar optical phonon scattering is found to be the important mechanism of scattering at high temperatures. The experimental results are discussed in the light of the calculated mobility.

© 2003 WILEY-VCH Verlag GmbH & Co. KGaA, Weinheim

### 1 Introduction

Over the past decade, GaN has been the focus of intense research [1–3]. Due to its large band gap, tunable between 1.9 and 6.2 eV upon alloying with In or Al, and its high thermal conductivity and stability GaN is ideally suited for making light-emitting diodes, lasers and detectors operating in the visible to ultraviolet range as well as high-power transistors with operating frequencies in the microwave region [4–6]. Compared with their technological applications, partly due to poor material quality, fundamental research on nitrides, particularly in electronic transport, appears to be in its infancy. For example, the rapid advance in fabricating high-quality sub-micrometre group III nitride modulation-doped field effect transistors [7] calls for reliable and predictive device simulations. While published transport studies of nitride compounds have so far focused on bulk properties [8–10], the prediction of efficient AlGaIn/GaN heterostructure devices requires accurate modelling of quantum confinement effects of the carriers in the two-dimensional (2D) channels. This is a prerequisite for understanding, predicting and optimising the effects of remote doping, interface roughness or temperature dependence [11, 12] of the electron mobility.

In modulation-doped structures a two-dimensional electron gas (2DEG) is formed at an AlGaIn/GaN heterointerface due to the electron affinity difference between the two materials. The space charge at the heterointerface creates a very strong built-in electric field that causes significant band bending in the GaN region. This strong band bending results in the confinement of electrons into a quasi-triangular potential well. Therefore, carrier motion in the direction perpendicular to the interface is quantised, forming a set of bound states. Motion along the interface remains unhindered. Since electrons are spatially

\* e-mail: sozalp@balikesir.edu.tr

separated from ionised parent impurities, this type of doping technique helps to reduce the ionised impurity scattering.

In this paper we use simple analytical expressions for the determination of low-field mobility in a 2DEG confined in a triangular well, taking into consideration all major scattering mechanisms, including interface roughness (IFR), ionised impurity scattering by remote donors and due to interface charge, acoustic deformation potential scattering, piezoelectric scattering and polar optical phonon scattering, using 2D degenerate statistics of 2DEGs. Because the efforts at explaining the observed mobilities in AlGaIn/GaN modulation-doped heterostructures have not considered the IFR scattering [13–18], we also investigate the effect of IFR on the low-field mobility of 2DEGs at low temperatures. The IFR scattering is typically quantified on the basis of weak perturbation theory in terms of two parameters: the lateral size ( $\Delta$ ) and the correlation length ( $\Lambda$ ) between fluctuations [19–26]. These parameter values affect the transport properties of 2DEGs at low temperatures. The principal objective of all theoretical calculations of 2D transport is to understand the scattering mechanisms limiting electron mobilities in such structures. The point of the theory is to provide an accurate description of the electronic structure of electrons confined in a quasi-triangular quantum well at the heterointerface. Section 2 discusses the mobility calculations in detail. The results of the calculations as well as their relation to experimentally obtained mobilities are the focus of Section 3. Finally, we summarize our results in Section 4.

## 2 Scattering mechanisms

The scattering theories of the 2D carriers in III–V heterojunction systems have been well developed by several authors [27–33]. The dominant scattering mechanisms for the 2D and bulk III–V compounds are now well established [34]. In our calculations of electron mobility in the 2DEG in the GaN/AlGaIn heterojunction we include IFR, impurity scattering by remote donors and due to interface charge, acoustic deformation potential scattering, piezoelectric scattering and polar optical phonon scattering. We consider the degenerate statistics of 2DEGs for the lowest subband occupation for the structure, as shown in Fig. 2.

The analytical expressions for the above mentioned scattering mechanisms are briefly summarized below for convenience and the material parameters used in the calculations are also listed in Table 1.

### 2.1 Ionised impurity scattering due to remote donors

At low temperatures, the electron mobility is limited by the ionised remote impurity scattering by remote parent donors in the barrier separated from the channel by a thin spacer layer. The value of the mobility limited by this scattering mechanism is given by [35, 36]

$$\mu_1 = \frac{64\pi\hbar^3 \varepsilon S_0^2 (2\pi n_s)^{3/2}}{e^3 m^*} \left[ \frac{1}{(Z_0)^2} - \frac{1}{(d_1 + Z_0)^2} \right]^{-1} \quad (1)$$

where  $\varepsilon$  is the dielectric constant of the crystal,  $\hbar$  is the reduced Planck constant,  $m^*$  is the electron effective mass,  $n_s$  is the density of the 2D electron gas,  $Z_0$  is the width of the quantum well and  $d_1$  is the

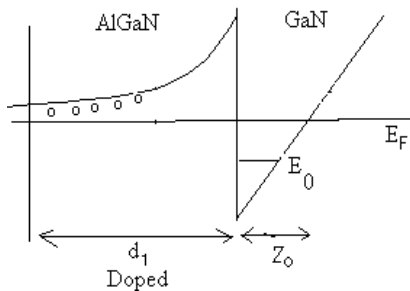


**Fig. 1** Energy and band diagram of a modulation-doped heterojunction.  $d_1$  is the width of the depletion layer and  $Z_0$  is the average distance of the electronic wave function from the heterointerface corresponding to the lowest subband.

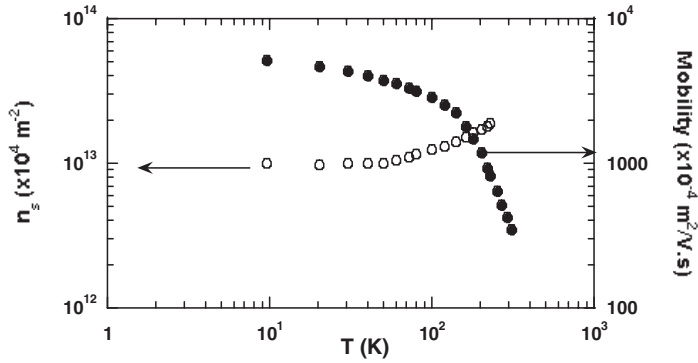


**Fig. 2** Two-dimensional electron density (open circles) and Hall mobility (filled circles) versus temperature.

width of the depletion layer. The screening constant  $S_0$  is a function of  $n_s$  and the lattice temperature  $T_L$ , which is given in the non-degenerate case by [28]

$$S_0 = \frac{e^2 n_s}{2\epsilon k T_L} \quad (2)$$

and in the degenerate case by

$$S_0 = \frac{e^2 m^*}{2\pi\epsilon\hbar^2}. \quad (3)$$

Since impurity scattering dominates only at low temperatures, the degenerate limit should be used for  $S_0$ .  $d_1$  is given by the approximation as  $d_1 = n_s/N_d$ , where  $N_d$  is the donor density in the barrier.

## 2.2 Ionised impurity scattering due to interface charge

Since the 2DEG is formed on the GaN side of the (AlGa)N/GaN heterointerface, there is additional scattering due to background impurities, the density of which is of the order of  $10^{14} \text{ cm}^{-3}$ , as well as due to

**Table 1** Values of GaN material constants used in the calculations.

electron effective mass	$m^* = 0.22m_0$
high-frequency dielectric constant	$\epsilon_\infty = 5.35$
static dielectric constant	$\epsilon_s = 9.7$
LO phonon energy	$\hbar\omega = 92 \text{ meV}$
width of the quantum well	$Z_0 = 65 \text{ \AA}$
longitudinal acoustic phonon velocity	$u_l = 6.56 \times 10^3 \text{ m s}^{-1}$
transverse acoustic phonon velocity	$u_t = 2.68 \times 10^3 \text{ m s}^{-1}$
density of the crystal	$\rho = 6.15 \times 10^3 \text{ kg m}^{-3}$
deformation potential	$E_d = 8.3 \text{ eV}$
dielectric constant of the crystal	$\epsilon = 8.58 \times 10^{-11} \text{ F m}^{-1}$
donor density	$N_d = 3 \times 10^{24} \text{ m}^{-3}$
density of the 2DEG	$n_s = 1 \times 10^{17} \text{ m}^{-2}$
width of the depletion layer	$d_1 = 3.33 \times 10^{-8} \text{ m}$
impurity density	$N_{BI} = 1 \times 10^{20} \text{ m}^{-3}$
piezoelectric constant	$h_{14} = 0.375 \text{ C m}^{-2}$
electron wavevector	$k = 7.3 \times 10^8 \text{ m}^{-1}$

the interface charge [37]. The corresponding mobility  $\mu_{\text{BI}}$  is given by [36]

$$\mu_{\text{BI}} = \frac{8\pi\hbar^3 \varepsilon^2 k_{\text{F}}^2 I_{\text{B}}(\beta)}{e^3 m^{*2} N_{\text{BI}}} \quad (4)$$

where  $N_{\text{BI}}$  is the 2D impurity density in the potential well due to background impurities and/or interface charge and

$$I_{\text{B}}(\beta) = \int_0^{\pi} \frac{\sin^2 \theta \, d\theta}{(\sin \theta + \beta)^2} \quad (5)$$

where

$$\beta = S_0/2k_{\text{F}} \quad (6)$$

and  $k_{\text{F}}$  is the wavevector on the Fermi surface.

### 2.3 Acoustic deformation potential scattering

When the temperature increases, the electron mobility depends on the acoustic phonon scattering. The mobility limited by this scattering mechanism is given by [38]

$$\mu_{\text{A}} = \frac{2e\hbar^3 \rho u_{\text{t}}^2 Z_0}{3m^{*2} E_{\text{d}}^2 k_{\text{B}} T_{\text{L}}} \quad (7)$$

where  $\rho$  is the density of the crystal,  $u_{\text{t}}$  is the longitudinal acoustic phonon velocity,  $Z_0$  and  $E_{\text{d}}$  are the effective width of the 2DEG and the deformation potential constant, respectively, as shown in Fig. 1, and  $k_{\text{B}}$  is the Boltzmann constant.

### 2.4 Piezoelectric scattering

At intermediate temperatures, the electron mobility is related to piezoelectric scattering in the 2DEG as [28]

$$\mu_{\text{PE}} = \frac{\pi k_{\text{F}} E_{\text{d}}}{Z_0 e h_{14}^2} \left[ \frac{1}{\frac{9}{32} + \frac{13}{32} \left( \frac{u_{\text{t}}}{u_{\text{l}}} \right)^2 \frac{I_{\text{A}}(\gamma_{\text{t}})}{I_{\text{A}}(\gamma_{\text{l}})}} \right] \mu_{\text{A}} \quad (8)$$

where  $h_{14}$  is the piezoelectric constant,  $u_{\text{t}}$  is the velocity of transverse acoustic phonons and

$$k_{\text{F}} = (2\pi n_{\text{s}})^{1/2} \quad (9)$$

$$I_{\text{A}}(\gamma_{\text{t}}) = \left[ \left( \frac{4\gamma_{\text{t}}}{3\pi} \right)^2 + 1 \right]^{1/2} \quad (10)$$

$$I_{\text{A}}(\gamma_{\text{l}}) = \left[ \left( \frac{4\gamma_{\text{l}}}{3\pi} \right)^2 + 1 \right]^{1/2} \quad (11)$$

$$\gamma_{\text{t}} = \frac{2\hbar u_{\text{t}} q_{\text{F}}}{k_{\text{B}} T} \quad (12)$$

$$\gamma_{\text{l}} = \frac{2\hbar u_{\text{l}} q_{\text{F}}}{k_{\text{B}} T}. \quad (13)$$

### 2.5 Polar optical phonon scattering

At high temperatures, the mobility of the carriers is limited by the polar optical phonon scattering that is comparable to acoustic deformation potential and piezoelectric scattering. The expression of mobility limited by the polar optical phonon is [31]

$$\mu_{\text{PO}} = \frac{4\pi\epsilon_p\hbar^2}{e\omega m^{*2} Z_0} \left[ \exp\left(\frac{\hbar\omega}{k_B T}\right) - 1 \right] \epsilon_0 \quad (14)$$

where

$$\frac{1}{\epsilon_p} = \frac{1}{\epsilon_\infty} - \frac{1}{\epsilon_s},$$

in which  $\epsilon_\infty$  and  $\epsilon_s$  are the dielectric constants of the semiconductor at high and low frequencies, respectively, and  $\hbar\omega$  is the optical phonon energy.

### 2.6 IFR scattering

IFR in layered structures can be in the form of well width fluctuations or alloy fluctuations both leading to the perturbation of the electron confinement energy [39–41]. The presence of IFR in optical devices can lead to some undesirable effects such as the splitting or broadening of excitonic spectra. The effect is more prominent in narrower wells where a few monolayer fluctuations in the well width result in a large fluctuation in the quantised energy [42]. The effect of IFR is also observed in conventional longitudinal transport measurements [43]. The carrier transport in quantum wells is mainly limited by IFR scattering [44]. Furthermore, at high electric fields, the IFR scattering of non-equilibrium LO phonons can render the non-drift hot phonon population, leading to the saturation of the high-field electron drift velocity and inhibition of negative differential resistance (NDR) [45, 46].

The influence of IFR on the mobility of 2D electrons in modulation-doped GaN/AlGaIn quantum wells is never very precise since the roughness itself is not straightforward to model. In this section, we adopt an approach commonly used for its mathematical convenience by other workers [45–48], namely we assume that fluctuations in the interface position are randomly correlated spatially, the correlation being describable by a Gaussian distribution. As regards the interaction we assume a variation in the potential that the electron experiences to be based on a first-order Taylor expansion of the confining potential [48–50]:

$$\Delta V(\mathbf{r}) = \frac{e^2 n_s}{2\epsilon_s} \Delta(\mathbf{r}). \quad (15)$$

Taking this as the perturbation we assume a correlation of the form

$$\langle \Delta(\mathbf{r}) \Delta(\mathbf{r}') \rangle = \Delta^2 \exp\left[-\frac{(\mathbf{r} - \mathbf{r}')^2}{\Lambda^2}\right] \quad (16)$$

where  $\mathbf{r}$  and  $\mathbf{r}'$  are the 2D spatial coordinates. Therefore, the mobility of electrons being scattered from IFR is obtained as

$$\mu_{\text{IFR}} = \frac{e}{m^*} \left[ \left( \frac{e^2 n_s \Delta \Lambda}{2\epsilon_s} \right)^2 \frac{m^*}{\hbar^3} J(k) \right]^{-1} \quad (17)$$

where

$$J(k) = \int_0^{2k} \frac{\exp(-q^2 \Lambda^2 / 4)}{2k^3 (q + q_s)^2 \sqrt{1 - (q/2k)^2}} q^4 dq, \quad (18)$$

$q = 2k \sin(\theta/2)$ ,  $k$  is the electron wavevector,  $\theta$  is the scattering angle and  $q_s$  is the screening constant given by [43]

$$q_s = \frac{e^2 m^*}{2\pi\epsilon_s \hbar^2} F(q) \quad (19)$$

in which  $F(q)$  is the form factor defined by [43]

$$F(q) \equiv \int_0^\infty dz \int_0^\infty dz' [f(z)]^2 [f(z')]^2 \exp(-q|z-z'|) \quad (20)$$

where  $f(z)$  is the Fang–Howard variational wave function [30].

### 3 Electron mobilities in AlGaIn/GaN modulation-doped heterostructures

The sample investigated in this work was grown using MBE on tungsten-backed sapphire substrates. The thickness of the  $\text{Al}_{0.15}\text{Ga}_{0.85}\text{N}$  barrier is 250 Å and has a doping density of  $3 \times 10^{18} \text{ cm}^{-3}$ . In order to see the relative importance of the various scattering mechanisms described above in determining the total mobility, we first present in Fig. 2 the temperature dependence of the 2DEG mobility and carrier density between lattice temperatures  $T_L = 10$  and 300 K. Figure 2 shows that the mobility is  $\mu = 5153.7 \text{ cm}^2/\text{V s}$  at 10 K and  $\mu = 348.51 \text{ cm}^2/\text{V s}$  at 300 K.

A basic mobility characteristic of the modulation-doped heterostructure, which reveals the importance of the different mechanisms, is the temperature dependence of the electron mobility. Figure 3 depicts the calculated low-field drift mobilities of the electrons in the channel as a function of temperature. The triangles represent the drift mobility calculated from Matthiessen's rule for the sample with doping concentration of  $3 \times 10^{18} \text{ cm}^{-3}$ . This density yields a sheet charge density of  $1 \times 10^{13} \text{ cm}^{-2}$  in the channel. We find the corresponding drift mobility of 2D electrons in the GaN channel to be  $358.37 \text{ cm}^2/\text{V s}$  at room temperature and  $8685.7 \text{ cm}^2/\text{V s}$  at 10 K. It is clear that at room temperature, polar optical phonon scattering is the dominant scattering mechanism. On the other hand, at intermediate temperatures, electron mobility is limited by deformation potential acoustic and piezoelectric acoustic scatterings. At low temperatures, the ionised impurity scattering is independent of temperature, with the constant mobility value of  $\mu_i = 10130 \text{ cm}^2/\text{V s}$ .

It is clear that the calculated mobilities at room temperature agree well with the experimental results. However, at low temperatures, the calculated values are higher than the experimentally determined mobilities. The reason for this discrepancy may be associated with IFR scattering and dislocation scattering. In this paper, we focus on IFR scattering. Our efforts on scattering by dislocations for explaining the

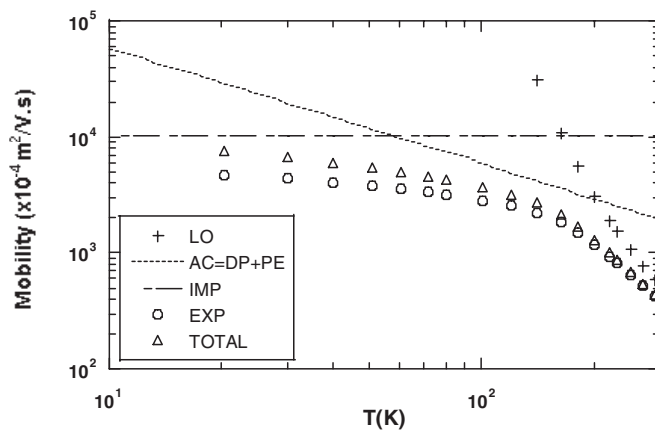


**Fig. 3** Calculated 2D electron mobility versus temperature for GaN/AlGaIn. Triangles represent calculated values from Matthiessen's rule; LO: optic phonon; AC: acoustic phonon; DP: deformation potential; PE: piezoelectric; IMP: remote and background impurities; TOTAL: calculated mobility from Matthiessen's rule.

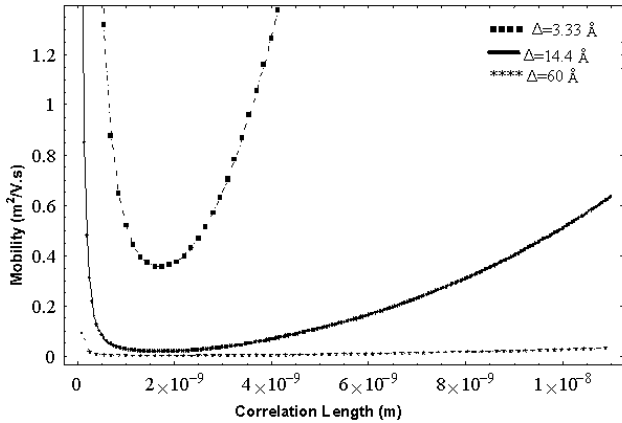


**Fig. 4** Calculated 2D electron mobility limited by IFR as a function of correlation length  $\Lambda$  for interfaces of different roughness,  $n_s = 1 \times 10^{17} \text{ m}^{-2}$  and  $T = 4.2 \text{ K}$ , using a Gaussian distribution.

observed mobility will be reported in a future paper. IFR scattering can dominate the low-temperature mobility of 2D electrons in GaN/AlGaIn structures with a high electron density since a small roughness of the heterointerfaces can cause a large fluctuation in the quantisation energy of confined 2D electrons [51–54]. In order to confirm such an interpretation, Fig. 4 shows mobility versus correlation length for three values of the well width fluctuation  $\Delta$  at a lattice temperature of 10 K. A good agreement with the experimental mobility  $\mu = 5153.7 \text{ cm}^2/\text{V s}$  is evident when we use a correlation length of  $\Lambda = 100 \text{ \AA}$  for a lateral size well width fluctuation of  $\Delta = 14.4 \text{ \AA}$  and for the experimental carrier concentration  $n_s = 1 \times 10^{17} \text{ m}^{-2}$ . For the same carrier concentration mobilities similar to the experimental ones can also be obtained by choosing a different set of lateral size and correlation length values, such as  $\Delta = 66 \text{ \AA}$ ,  $\Lambda = 200 \text{ \AA}$  and  $\Delta = 3.33 \text{ \AA}$ ,  $\Lambda = 50 \text{ \AA}$ , as indicated in Fig. 4.

Figure 5 shows the calculated mobility as a function of carrier concentration for different IFR parameters. It is clear that the mobility decreases with increasing carrier concentration and that the mobility is more sensitive to the magnitude of the IFR parameters for lower carrier densities. Therefore, IFR scattering at these high carrier concentrations is the dominant mechanism, which affects the transport properties of the 2DEG at low temperatures.

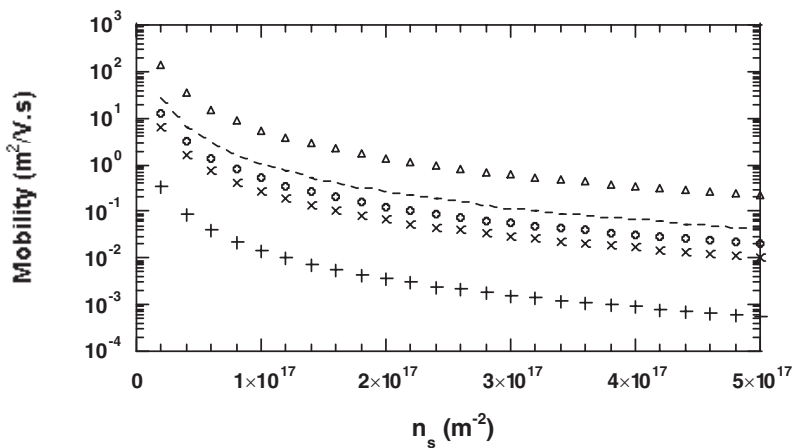


**Fig. 5** Calculated 2D electron mobility limited by IFR as a function of sheet electron density for interfaces of different roughness using a Gaussian distribution:  $\circ$   $\Lambda = 100 \text{ \AA}$ ,  $\Delta = 14.4 \text{ \AA}$ ;  $-$   $\Lambda = 100 \text{ \AA}$ ,  $\Delta = 10 \text{ \AA}$ ;  $\times$   $\Lambda = 100 \text{ \AA}$ ,  $\Delta = 20 \text{ \AA}$ ;  $\Delta$   $\Lambda = 200 \text{ \AA}$ ,  $\Delta = 20 \text{ \AA}$ ;  $+$   $\Lambda = 50 \text{ \AA}$ ,  $\Delta = 20 \text{ \AA}$ .

## 4 Conclusion

In this paper we compare the experimentally determined Hall mobility of a 2DEG formed at an AlGaIn/GaN heterointerface with theory. In the theory all major scattering mechanisms, including IFR scattering, ionised impurity scattering, acoustic deformation potential scattering, piezoelectric scattering and polar optical phonon scattering, have been taken into account. The temperature dependence of the observed mobility is explained very well by the temperature-independent ionised impurity and IFR and by the temperature-dependent acoustic deformation potential, piezoelectric and polar optical phonon scattering. We show that IFR scattering limits mobility in AlGaIn/GaN modulation-doped heterointerfaces with a high electron density,  $n_s > 10^{12} \text{ cm}^{-2}$ , at low temperatures.

## References

- [1] R. Gaska, M. S. Shur, A. D. Bykhovski, A. O. Orlov, and G. L. Snider, *Appl. Phys. Lett.* **74**, 287 (1999).
- [2] S. Nakamura, T. Mukai, and M. Senoh, *Appl. Phys. Lett.* **64**, 1687 (1994).
- [3] R. Gaska, Q. Chen, J. Yang, A. Osinsky, M. A. Khan, and M. S. Shur, *IEEE Electron Dev. Lett.* **18**, 492 (1997).
- [4] T. D. Moustakas, J. H. Pankove, and Y. Hamakawa, (eds.) *Wide Band Gap Semiconductors*, Symp. Proc. No. 242 (Materials Research Society, Pittsburgh, 1992).
- [5] Van de Walle, ed., *Wide Band Gap Semiconductors*, Proc. 7th Trieste Semiconductor Symp. (North-Holland, Amsterdam, 1993); *Physica B* **185** (1993).
- [6] S. Nakamura, T. Muaki, and M. Senoh, *J. Appl. Phys.* **76**, 8189 (1994).
- [7] Y. F. Wu, B. P. Keller, S. Keller, D. Kapolnek, P. Kozodoy, S. P. Denbaars, and U. K. Mishra, *Appl. Phys. Lett.* **69**, 1438 (1996).
- [8] B. E. Foutz, L. F. Eastman, U. V. Bhapkar, and M. S. Shur, *Appl. Phys. Lett.* **70**, 2849 (1997).
- [9] R. P. Joshi, *Appl. Phys. Lett.* **64**, 223 (1994).
- [10] J. Kolnik, I. H. Oğuzman, K. F. Brennan, R. Wang, and P. P. Ruden, *J. Appl. Phys.* **78**, 1033 (1996).
- [11] U. V. Bhapkar and M. S. Shur, *J. Appl. Phys.* **82**, 1649 (1997).
- [12] Q. Chen, A. M. Khan, J. W. Yang, C. J. Sun, M. S. Shur, and H. Park, *Appl. Phys. Lett.* **69**, 794 (1996).
- [13] L. Hsu and W. Walukiewicz, *Phys. Rev. B* **56**, 1520 (1997).
- [14] O. Aktas, Z. F. Fan, S. N. Mohammad, A. E. Botchkarev, and H. Morkoç, *Appl. Phys. Lett.* **69**, 3872 (1996).
- [15] K. Hirakawa and H. Sakaki, *Phys. Rev. B* **33**, 8291 (1986).
- [16] R. Oberhuber, G. Zandler, and P. Vogl, *Appl. Phys. Lett.* **73**, 818 (1998).
- [17] V. K. Arora and A. Naeem, *Phys. Rev. B* **31**, 3887 (1985).
- [18] K. Lee, M. S. Shur, T. J. Drummond, and H. Morkoç, *J. Appl. Phys.* **54**, 6432 (1983).
- [19] F. Stern, *Phys. Rev. Lett.* **44**, 1469 (1980).
- [20] A. J. Sirekowsky and L. F. Eastman, *J. Appl. Phys.* **86**, 3398 (1999).
- [21] B. K. Ridley, *Appl. Phys. Lett.* **77**, 990 (2000).
- [22] T. J. Drummond, H. Morkoc, and A. V. Cho, *J. Appl. Phys.* **52**, 1380 (1981).
- [23] H. L. Stormer, A. V. Gossard, and W. Wiegman, *Appl. Phys. Lett.* **39**, 493 (1981).
- [24] R. Dingle, H. L. Stormer, A. C. Gossard, and W. Wiegman, *Appl. Phys. Lett.* **33**, 665 (1978).
- [25] T. J. Drummond, W. Kopp, M. Keever, H. Morkoc, and A. Y. Cho, *J. Appl. Phys.* **53**, 1023 (1982).
- [26] H. Sakaki, T. Noda, K. Hirakawa, M. Tanaka, and T. Matsusue, *Appl. Phys. Lett.* **51**, 1987 (1987).
- [27] P. J. Price, *Ann. Phys. (NY)* **133**, 578 (1982).
- [28] K. Lee, M. S. Shur, T. J. Drummond, and H. Morkoc, *J. Appl. Phys.* **54**, 6432 (1983).
- [29] W. Walukiewicz, H. E. Ruda, J. Lapowski, and H. C. Gatos, *Phys. Rev. B* **30**, 4571 (1984).
- [30] F. Stern, *Phys. Rev. B* **5**, 4891 (1972).
- [31] B. K. Ridley, *J. Phys. C* **15**, 5899 (1982).
- [32] E. E. Mendez, P. J. Price, and H. Heiblim, *Appl. Phys. Lett.* **45**, 294 (1984).
- [33] K. Hirakawa, H. Sakaki, and J. Yoshino, *Appl. Phys. Lett.* **45**, 253 (1984).
- [34] D. L. Rode, in: *Semiconductors and Semimetals*, edited by R. K. Willardson and A. C. Beer (Academic Press, New York, 1975), Chap. 1.
- [35] H. Mathieu, *Physique des Semiconducteurs et des Composants Electroniques* (Mason, 1997).
- [36] K. Hess, *Appl. Phys. Lett.* **35**, 484 (1979).
- [37] C. T. Sah, T. H. Ning, and L. L. Tschopp, *Surf. Sci.* **32**, 561 (1972).
- [38] K. V. Arora and A. Naeem, *Phys. Rev. B* **31**, 3887 (1985).
- [39] M. Tanaka and H. Sakaki, *J. Cryst. Growth* **81**, 513 (1987).



- [40] C. A. Warwick, W. J. Jan, and A. Ourmazd, *Appl. Phys. Lett.* **56**, 2666 (1990).
- [41] P. F. Fewster, N. L. Andrew, and C. J. Curling, *J. Appl. Cryst.* **21**, 524 (1988).
- [42] B. Deveaud, J. Y. Emergy, A. Chomette, B. Lambert, and M. Baudet, *Superlattices Microstruct.* **3**, 205 (1985).
- [43] K. Hirakawa and H. Sakaki, *Phys. Rev. B* **33**, 8291 (1986).
- [44] R. Gupta and B. K. Ridley, *Phys. Rev. B* **41**, 11972 (1993).
- [45] R. Gupta, N. Balkan, and B. K. Ridley, *Semicond. Sci. Technol.* **7B**, 274 (1992).
- [46] N. Balkan, R. Gupta, M. E. Daniels, B. K. Ridley, and M. Emeny, *Semicond. Sci. Technol.* **5**, 986 (1990).
- [47] B. K. Ridley, B. E. Foutz, and L. F. Eastman, *Phys. Rev. B* **61**, 16862 (2000).
- [48] H. Sakaki, T. Noda, K. Hirakawa, M. Tanaka, and T. Matsusue, *Appl. Phys. Lett.* **51**, 1934 (1987).
- [49] A. Gold, *J. Phys. B* **74**, 53 (1989).
- [50] N. Balkan, R. Gupta, M. Cankurtaran, H. Celik, A. Bayrakli, E. Tiras, and M. C. Arikan, *Superlattices Microstruct.* **22**, 263 (1997).
- [51] S. Hiyamizu, Fuji, T. Mimura, K. Nanbu, J. Saito, and H. Hashimoto, *Jpn. Appl. Phys.* **20**, L455 (1981).
- [52] A. Madhukar, *Surf. Sci.* **132**, 344 (1983).
- [53] R. Heckingbottom, G. J. Davies, and K. A. Prior, *Surf. Sci.* **B2**, 375 (1983).
- [54] G. Margaritondo, *Surf. Sci.* **132**, 469 (1983).